Published in final edited form as:
Invest Ophthalmol Vis Sci. 2009 May ; 50(5): 1996–2003. doi:10.1167/iovs.08-2556.

Multiple Genes on Chromosome 7 Regulate Dopaminergic Amacrine Cell Number in the Mouse Retina

Irene E. Whitney[1], **Mary A. Raven**[1], **Daniel C. Ciobanu**[2], **Robert W. Williams**[2], and **Benjamin E. Reese**[1]

1 *Neuroscience Research Institute and Department of Psychology, University of California, Santa Barbara, CA 93106*

2 *Department of Anatomy and Neurobiology, University of Tennessee Health Science Center, Memphis, TN 38163*

Abstract

Purpose—The size of neuronal populations is modulated by gene variants that influence cell production and survival, in turn influencing neuronal connectivity, function, and disease risk. The size of the dopaminergic amacrine (DA) cell population is a highly heritable trait exhibiting six-fold variation among inbred strains of mice, and is used here to identify genes that modulate the number of DA cells.

Methods—The entire population was counted in retinal wholemounts from 37 genetically defined lines of mice, including six standard inbred strains, 25 recombinant inbred strains (AXB/BXA), reciprocal F1 hybrids, a chromosome (Chr) 7 consomic line, and three additional genetically modified lines.

Results—We mapped much of this variation to a broad locus on Chr 7 (*Dopaminergic amacrine cell number control, Chr 7*). The *Dacnc7* locus is flanked by two candidate genes known to modulate the number of other types of retinal neuron—the pro-apoptotic gene, *Bax*, and tyrosinase. The *Tyr* mutation was shown to modulate DA cell number modestly, although in the direction opposite that predicted. In contrast, *Bax* deficiency increased the population four-fold. *Bax* expression was significantly greater in the A/J strain relative to C57BL/6J, an effect that may be due to an SNP in a p53 consensus binding site known to modulate transcription. Finally, we note a strong candidate situated at the peak of the *Dacnc7* locus, *Lrrk1*, a Parkinson's disease gene exhibiting mis-sense mutations segregating within the AXB/BXA cross.

Conclusions—Multiple polymorphic genes on Chr. 7 modulate the size of the population of DA cells.

Keywords

QTL; recombinant inbred strain; consomic strain; tyrosinase; Bax; Lrrk1; cell death

INTRODUCTION

Natural variation in neuronal number between individuals is a product of environmental determinants and genetic variants that modulate the processes of cellular production and survival. Inbred strains of mice provide an excellent resource with which to examine each

Corresponding author: B. E. Reese, Neuroscience Research Institute, University of California, Santa Barbara, CA 93106-5060; phone & fax: 805-893-2091; email: E-mail: breese@psych.ucsb.edu.

separately, by looking at the phenotypic differences within an isogenic line, or by comparing the phenotypic variance between different lines of mice. The latter approach has made it possible to uncover chromosomal loci that contribute to differences in brain structure and neuronal number in a variety of regions within the central nervous system, from which one can identify candidate polymorphic genes existing between such strains that may be directly responsible for this genetic component in the phenotypic variation[1–5].

The success in mapping such quantitative traits to genomic loci requires sufficient variability among strains in the absence of conspicuous inter-individual variability within a strain. The dopaminergic (DA) amacrine cells comprise less than one-hundredth of a percent of the total population of retinal neurons[6]. Remarkably, we show here that the number of DA amacrine cells in the retina is tightly conserved within a strain despite their meager absolute number, yet between strains there is a substantial variance in the size of this population. To identify gene variants that modulate the number of DA amacrine cells, we used recombinant inbred strains derived from the A/J and C57BL/6J (B6/J) laboratory strains. We provide evidence for a broad quantitative trait locus (QTL) on chromosome 7 controlling DA cell number, and identify three candidate genes, two of which, when disrupted, modulate the size of this population, and the third of which is associated with Parkinson's disease.

METHODS

Six different inbred laboratory strains of mice [A/J, C57BL/6NCrl (hereafter B6/NCrl), C57BL/6J (hereafter B6/J), DBA2/J, ALR/LtJ and ALS/LtJ], twenty-five recombinant inbred (RI) strains derived from the A/J and B6/J strains (the AXB/BXA strain-set; see Supplementary Table 1), two F1 crosses (AB6F1/J and B6AF1/J), one chromosome substitution strain (C57BL/6J-Chr $7^{A/J}$NaJ; hereafter B6.A<7>), one strain possessing a point mutation in the *Tyr* gene (B6(Cg)-$Tyr^{c\text{-}2J}$/J) that is coisogenic with B6/J, one strain with a segment of Chr. 7 from B6/J introgressed onto an A/J background, including wildtype *Tyr* alleles (A.B6-$Tyr^{+/J}$), and one strain congenic with B6/J containing a targeted deletion of the *Bax* gene (B6.129X1-Bax^{tm1Sjk}/J) were obtained. B6/NCrl stock was ordered from Charles River Laboratories and bred in the Animal Resource Center at UCSB. All other stock was obtained from The Jackson Laboratory for immediate use or for use after a single generation. All experiments were conducted under authorization by the Institutional Animal Care and Use Committee at UCSB, and in accord with the NIH Guide for the Care and Use of Laboratory Animals and the ARVO Statement for the Use of Animals in Ophthalmic and Vision Research.

Mice were perfused with 2 ml of 0.9% saline followed by 50 ml of 4% paraformaldehyde in 0.1 M sodium phosphate buffer (pH 7.2 at 20°C). Whole retinas were dissected immediately, rinsed in phosphate buffer, and then immunolabeled at 4°C using standard indirect immunofluorescence techniques. All incubation solutions included 1% Triton-X100 in phosphate-buffered saline (PBS). Retinas were incubated in a blocking solution (5% normal donkey serum and 2% bovine serum albumin; Sigma; St. Louis, MO) for 3 hours and then rinsed with PBS. Retinas were then incubated in mouse monoclonal antibody to tyrosine hydroxylase (1:10,000; #T1299, Sigma) over three nights, rinsed in PBS, and incubated in donkey anti-mouse secondary antibody conjugated to Cy3 (1:200; #715-165-151, Jackson ImmunoResearch Labs; West Grove, PA) overnight. Retinas were rinsed with PBS followed by 0.1 M phosphate buffer.

Following rinses, retinas were mounted under a coverslip in phosphate buffer and examined using an Olympus BH2 fluorescence microscope coupled via a Sony video camera to a computer running Bioquant Nova Prime software (R&M Biometrics, Nashville, TN). The entire retinal wholemount was quantified (retinal wholemounts missing a small portion were excluded from the analysis), while plotting the position of every large, TH-immunoreactive

(i.e. dopaminergic) amacrine cell in the inner nuclear and ganglion cell layers (the latter are rare, as previously reported[7], amounting to less than 4 cells per retina). A minimum of three mice were sampled in each strain, the *n* being indicated within every bar in each histogram. The mean total number and standard error (SE) of DA cells in each strain is plotted in all histograms and described in the text, except at those locations in the text where the standard deviation within a population is specifically quoted. Individual fields for illustration were imaged using an Olympus Fluoview laser scanning confocal microscope with a 20× objective, in which image stacks were collected at 1 μm intervals.

QTL mapping was performed using the WebQTL mapping module of GeneNetwork (www.genenetwork.org). We mapped the loci that modulate DA cell number using a weighted interval mapping method that takes into account the significant differences in errors of strain means (see the function labeled "Use SE or Variance for Weighted Regression" toward the bottom of the Trait Data and Analysis Form), excluding the parental strains in the mapping. Following standard interval mapping, we also mapped residual differences in DA cell number using a composite interval procedure that controls for the confirmed presence of a locus on Chr 7. High-resolution consensus sequence maps are available for this RI strain-set[8, 9]. The phenotype data in this paper have been entered into the AXB/BXA Phenotypes database in GeneNetwork as record ID 10127. All megabase (Mb) position values in this paper refer to the Mouse Genome Assembly of 2006 (mm8).

WebQTL employs a permutation test of the RI strain data to determine the probability of achieving LRS scores by chance. Thresholds for suggestive and significant LRS scores are indicated in figures 3a and b. WebQTL also performs a bootstrap test of the RI strain data, examining the robustness of the site of the peak LRS. This is indicated in the yellow histogram of figure 3b. Both procedures are described in detail at (www.genenetwork.org; see Glossary).

We used *Bax* mouse DNA sequence available in GenBank (NM_007527) and designed primers to amplify (GoTaq Flexi DNA polymerase, Promega Corporation, Madison, WI) the entire *Bax* gene of the A/J and B6/J strains. We performed the reverse transcription of total RNA by using M-MuLV (Moloney Murine Leukaemia Virus) reverse transcriptase and hexanucleotide priming according to the manufacturer's protocol (GE Healthcare, Piscataway, NJ). We used RNA extracted from postnatal day (P)10 retinas of A/J and B6/J strains to amplify the 5′ cDNA ends using FirstChoice RLM-RACE (Ambion, Austin, TX) according to instructions of the manufacturer. We also amplified around 1kb upstream of the transcription start of *Bax*. We sequenced the PCR products and 5′ cDNA ends using BigDye Terminator v3.1 cycle sequencing reagents (Applied Biosystems, Foster City, CA) and ABI3130xl genetic analyzer instrument. We used Sequencher software (GeneCodes, version 4.8, Ann Arbor, MI) to assemble and align DNA sequences of A/J and B6/J and to identify polymorphisms.

To examine expression of *Bax* and *Lrrk1* during development, retinas were collected from multiple P1, P5 and P10 litters of the A/J and B6/J strains using RNase-free reagents and were then stored in RNAlater (#AM7024, Ambion) at −20°C. The retinas were disrupted for extraction using RNase-free plastic pestles and tubes (#749515-1500 and # 749510-1500, Kontes, Rochester, NY) and homogenized on QIAshredder columns (#79654, Qiagen, Valencia, CA). RNA was then extracted using an RNeasy Plus Mini kit (#74134, Qiagen) according to the manufacturer's instructions. RNA concentration was measured using the Nanodrop-1000 and the RNA integrity was verified using the Agilent 2100 Bioanalyzer. A total of 27 individual RNA samples were used to generate cDNA. 250 g of each sample were reverse transcribed using the iScript cDNA kit (#170-8891, BioRad, Hercules, CA). 10μl of PCR master mix [Final concentration 50mM KCl, 10mM Tris-HCl (pH 9.0 at 25°C), 2.5mM $MgCl_2$, 0.1% Triton X-100, 0.4mM dNTPs (#U1515, Promega Corporation), 0.20 units Platinum Taq DNA Polymerase (#10966, Invitrogen, Carlsbad, CA), 1X SYBR Green I

(#S-7563, Invitrogen) and 20nM Fluorescein (#170-8780, BioRad,)], including cDNA, were added to 10μl of 1μM sense and anti-sense primers for each reaction. Primers were designed using Beacon Designer v.7.01 (Premier Biosoft International, Palo Alto, CA) and purchased from Operon (Huntsville, AL). Each individual sample was pipetted in quadruplicate using the Biomek 2000 Laboratory Automation Work Station (Beckman Coulter, Fullerton, CA) for the *Bax* and *Lrrk1* primers, as well as four housekeeping genes. The BioRad MyiQ Single Color Real-Time PCR Detection System was used to perform PCR amplifications and to generate Ct values. Data were corrected for product size and the temperature at which it was analyzed. PCR efficiencies were corrected using LinReg PCR software v.7.2[10]. The geometric mean of the housekeeping genes was used to normalize average amounts calculated from quadruplicate reactions[11].

RESULTS

DA cell number varies between laboratory strains

Analysis of six inbred laboratory strains revealed a remarkable four-fold variation in DA cell number (figure 1a, b). All retinas stained consistently for DA cells and their processes across the full extent of the retina (figure 1a), discounting variation in immunolabeling as the source of this variation in cell number. Retinas of A/J contained the fewest DA cells, with an average of 261 ± 7.7 (SEM), whereas ALS/LtJ contained the most, with an average of 962 ± 11.9 (figure 1a). ALR/LtJ averaged 732 ± 13.3 cells and DBA2/J averaged 756 ± 7.3 cells. The two C57BL/6 sub-strains that we studied showed significant differences: that from the Jackson Laboratory, C57BL/6J (B6/J), had 617 ± 8.3 cells, whereas that from Charles River Laboratories, C57BL/6NCrl (B6/NCrl), had 470 ± 19.8 cells (Student's t-test; $p < 0.05$). The B6/NCrl stock was separated in 1951 from the Jackson Laboratory's stock at generation F32 and since has been maintained separately for almost 200 generations.

Note the small variance within any of the strains (figure 1b), the standard deviation averaging about 5% of the mean number of DA cells. The heritability estimate of this trait (h^2) calculated using Hegmann and Possidente's method[12], was 0.84 for the laboratory strains; that is, the variable *strain* accounts for most of the variance within the dataset. Such high heritability makes DA cell number a particularly attractive trait for genetic dissection.

We counted retinas of reciprocal F1 hybrids (AB6F1/J and B6AF1/J) generated by crossing the A/J and B6/J strains, two parental strains that differ approximately 2.5-fold in DA cell number. If gene variants modulating DA cell numbers acted in a purely additive and independent manner, then the F1 hybrids would have a population size close to the mid-parental value of 439 cells. Values for the two F1 hybrids were 509 ± 7.4 for AB6F1/J, and 505 ± 4.8 for B6AF1/J (figure 1b), suggesting a mild dominance deviation toward the value of the B6/J parent. If DA cell number were influenced by a parent-of-origin effect (e.g., imprinting, maternal environment, or a mitochondrial effect) then one would expect a difference between the reciprocal hybrids. In fact, no significant difference was detected (Student's t-test; $p > 0.05$).

Analysis of Recombinant Inbred (RI) strains indicates multiple polymorphic genes contribute to DA cell number

The AXB/BXA RI strain-set consists of 25 independent strains derived from reciprocal crosses between A/J and B6/J strains[8, 13]. We determined DA cell number within each RI strain (figure 2). As for the inbred laboratory strains, so the individual RI strains also showed low within-strain variance, with an average coefficient of variation of 6%. Strain means for the 25 AXB/BXA RI strains, by contrast, were highly variable. Retinas of AXB12 contained merely 160 ± 20.0 cells whereas BXA12 contained 637 ± 4.3 cells. This variation was unrelated to either the

age of animals ($r = 0.017$, range from 25 to 88 days), or to total retinal area ($r = 0.047$, range from 14.11 to 19.31 mm^2). The wide range of variation that extends beyond the parental values, and the fact that the distribution was not obviously bimodal or multimodal, suggests that allelic variants in multiple genes participate in the regulation of DA cell number.

QTL mapping reveals a locus on chromosome 7

We mapped variation in DA cell number (see GeneNetwork AXB Phenotype ID 10127) using interval mapping and detected significant linkage on Chr 7 between 45 and 100 Mb (figure 3a). In this interval, the *B* allele has the anticipated effect on DA cell number, being an additive effect of approximately 65 DA cells per allele. The correlation between variation in DA cell number (strain means) and SNP genotypes at rs6160140 is 0.7, indicating that this single locus can account for up to 50% of the total genetic variance in DA cell number segregating in the AXB/BXA cross. This is a remarkably strong effect, and the presence of *B* alleles at this locus accounts for as much as 36% of the difference that we have detected between the parental strains. The Chr 7 locus, which we have named *Dopaminergic amacrine cell number control, Chr 7* (*Dacnc7*) was detected whether we mapped using conventional Haley-Knott linear regression equations, or using a weighted regression procedure implemented in WebQTL that factors in the standard error of the mean for each strain.

Consomic B6.A<7> mice confirm the presence of the QTL

Singer, Nadeau and colleagues have generated a series of chromosome substitution strains in which entire chromosomes from A/J have been introgressed onto a B6/J background[14]. We phenotyped the Chr 7 line (B6.A<7>) that has a complete A/J Chr 7 on an otherwise B6/J genetic background. This B6.A<7> consomic strain had an average of 509 ± 12.0 DA cells, or approximately 108 cells fewer than observed in the B6/J strain (figure 4). These results confirm the presence of the QTL on Chr 7. The size of this effect is about 83% that expected from the additive effect detected in the AXB/BXA cross; a reasonable concordance with expectation. This result strongly supports *Dacnc7* as a locus on Chr 7 that accounts for about one-third of the phenotypic difference between the parental strains.

In addition to *Dacnc7*, we also detected several secondary loci by composite interval mapping on Chr 3, 4, 9, and 15 (not shown). None of these intervals achieve statistical significance. However, an interval on Chr 9 centered at about 65 Mb near *Rora* (RAR-related orphan receptor alpha) is of some interest. The *B* allele in this interval is associated with lower numbers of DA cells. While such an "*A*-high" interval cannot explain the pronounced difference between parental phenotypes, it can help explain the observation that some of the AXB/BXA strains have numbers that are either lower or higher than the parental strains.

The AXB/BXA RI strain-set is comparatively small, and as a result, the 2-LOD score confidence interval of the QTL of Chr 7 is large and extends from about 45.5 to 100.8 Mb (figure 3b). This locus likely contains multiple polymorphic genes that affect DA cell number. Bootstrap re-samples of the strain phenotypes revealed approximately 60% that had a peak LRS score near 67 Mb, but the remaining 40% were scattered throughout the locus, consistent with this interpretation (yellow bars in figure 3b). We proceeded to examine two particularly attractive candidates flanking the center of *Dacnc7*.

Disrupting tyrosinase gene function modulates DA cell number

The distal region of *Dacnc7* contains one strong candidate gene that is already known to modulate cell proliferation in the retina, the *tyrosinase* (*Tyr)* gene. The mouse *Tyr* gene is located at 87.3 Mb (indicated in figure 3b), being on the fringe of the *Dacnc7* locus, but still a gene worthy of attention. *Tyr* encodes the enzyme tyrosinase, critical for the synthesis of melanin in the skin, hair, and eyes. Mutations in *Tyr* produce oculo-cutaneous albinism

(OCA1). Ocular hypopigmentation has been associated with abnormalities in cell division and in cell-cycle kinetics during retinal development[15–17] and in the number of certain types of retinal neurons at maturity[18, 19], raising the possibility that variants of this gene also modulate the production of DA cells. Wildtype B6/J mice contain a functional *Tyr* gene, while A/J contains a point mutation rendering *Tyr* non-functional, producing the albino phenotype. We consequently examined B6 (Cg)-*Tyr*$^{c\text{-}2J}$/*J* (albino) mice. This sub-strain is coisogenic with B6/J except for the presence of a distinct, spontaneously arising, point mutation at the Jackson Laboratory that also inactivates *Tyr*[20]. DA cell number was unexpectedly increased significantly by 63 cells (figure 5a; Student's t-test; $p < 0.01$), rather than being decreased, suggesting that the effect of the mutation in *Tyr* within A/J is masked by other alleles present within the QTL that lower DA cell number. Effects of the *Tyr* null mutation in A/J could also contribute to the observation that the consomic B6.A<7> strains had slightly higher DA neurons (about 20) than expected given the effect size of *Dacnc7*.

Congenic A.B6-Tyr$^{+/J}$ mice confirm other loci in the distal QTL modulate DA cell number

The wildtype *Tyr* allele has been backcrossed for more than ten generations to A/J, to yield a pigmented A.B6 congenic line. This strain was genotyped to determine the precise extent of the chromosomal interval around the *Tyr* gene that is derived from B6/J. A 55 Mb segment encompassing *Tyr* (from 73.8 to 122.3Mb) was confirmed to contain *B* alleles (figure 3b, shaded region). When compared with A/J, these congenic mice contained 86 more DA amacrine cells (figure 5b), a statistically significant increase (Student's t-test; $p < 0.01$). Because the B6 (Cg)-*Tyr*$^{c\text{-}2J}$/*J* mice had more DA cells than did the wildtype (pigmented) B6/J mice, the increase in DA cell number in the A.B6-*Tyr*$^{+/J}$ mice is unlikely to be due to the effect of the *Tyr*$^{+/+}$ alleles, indicating some other polymorphic gene (or genes) in the distal half of the QTL, yet to be identified, contributes to this phenotypic difference between the parental strains.

A gene in the proximal portion of the QTL modulates DA cell number

Another noteworthy candidate within the QTL is the gene for the *Bcl2* associated X protein, *Bax*, positioned proximal to the introgressed segment in the A.B6-*Tyr*$^{+/J}$ strain, at 45.3 Mb (also indicated in figure 3b). *Bax* is a pro-apoptotic gene that antagonizes the action of *Bcl2*, regulating the release of cytochrome c from the mitochondrion, and leading to the induction of apoptosis[21]. *Bcl2* overexpressing transgenic mice are known to have an excessive number of DA amacrine cells as well as other retinal neurons[22], while *Bax*$^{-/-}$mice have reduced levels of apoptosis and thicker ganglion cell and inner nuclear layers[23, 24]. We consequently examined the effect of knocking out *Bax* gene function upon DA cell number. *Bax*$^{-/-}$ mice showed a conspicuous increase in their number of DA cells, having an average of 2696 ± 140.8 cells, while the *Bax*$^{+/+}$ and *Bax*$^{+/-}$ littermate mice had numbers of DA cells that are comparable to the parental B6/J strain, being less than one quarter of this number (figure 6).

To investigate whether polymorphisms in the *Bax* gene may contribute to this natural variation in DA cell number between the A/J and B6/J strains, we sequenced the entire *Bax* gene from 45,329,773 to 45,334,934 Kb in both strains. We found three additional SNPs and a polymorphic STR (short tandem repeat). These polymorphisms, their locations and the alleles for each strain are listed first in Supplementary Table 2 and are followed by a previously identified SNP. All these polymorphisms were located in introns. The STR and two of the SNPs are part of low complexity DNA sequences and less likely to be part of any potential regulatory element.

We also investigated if the A/J and B6/J strains are using the same start site for *Bax* transcription, and if there are any structural differences between the *Bax* transcripts at the 5′ end. We were encouraged to look at this potential difference due to an interesting 5′ end

alternative transcript (AY095934) expressed in P3×63-Ag8.653 cell line (genome.ucsc.edu). Sequencing of the 5′ cDNA ends did not reveal any difference between the strains relative to the transcription start site nor structural differences at the 5′ end.

We did, however, find a difference in *Bax* gene expression throughout postnatal development using real time RT-PCR. mRNA was extracted from whole dissected A/J and B6/J retinas at postnatal day (P) 1, P5 and P10. A two-way ANOVA confirmed this effect of strain to be significant ($p < 0.01$), yet revealed no significant effect of age, nor the presence of any interaction (figure 7). This difference in *Bax* expression, in the direction predicted, suggests that regulatory variants within the *Bax* promoter segregate in the AXB RI panel. To examine this possibility, we sequenced the DNA upstream of the transcription start of *Bax* and uncovered an informative SNP (rs31477291) at the position – 475bp. The SNP variant of B6/J abolishes a perfect p53 binding site which is otherwise present in A/J[25].

DISCUSSION

The present results show tremendous variation in DA cell number across different strains of mice in the absence of substantial variation within any individual strain. There are two significant implications of these results: First, there should be polymorphic genes contributing to this natural variation between strains, and we have confirmed that this is the case by identifying a significant QTL on Chr 7, *Dacnc7*. Second, the specification of DA cell number within any strain of mice must be precisely controlled. We will consider each of these separately, in reverse order:

The specification of DA cell number shows a remarkable level of precision when one considers the fact that developmental mechanisms produce an excess of six million nerve cells in mouse retina[26]. Somehow, a small fraction of one percent of the cells exiting the cell cycle gets assigned to a DA cell fate. Subsequently, some proportion of these cells is eliminated during normal development to yield the final number of DA cells. The manner by which fate determining events and/or cell survival decisions might reproducibly yield a periodic patterning of even a sparse number of nerve cells is not hard to envision[27, 28], but the DA cells do not conform to a regular array in the mouse retina. Rather, they are nearly random in their local distribution, but for the operation of a large exclusion zone reducing the tendency of close-neighbor pairings[7]. Such exclusion zones are often sufficient for producing regularity in nerve cell patterning[29, 30], but in the case of the DA cells, their packing is still far below the theoretical packing limit imposed by such an exclusion zone, yielding regularity indexes close to those generated by random simulations[7]. Consequently, it remains intriguing how fate determination events and cell survival processes produce such tightly defined numbers of DA cells in the absence of any precise patterning in their spatial distribution.

The present results show that Chr 7 contains multiple genes that influence DA cell number. *Tyr* and another nearby gene (or genes) antagonize one another in their effect upon DA cell number, while more proximally, *Bax* gene function has been shown to have a profound effect upon DA cell number. *Tyrosinase*-mutant mice are known to have altered cell-cycle kinetics and reductions in some[16, 18, 19, 31, 32], if not all, retinal cell types[33], so the fact that DA cell number was increased in the $Tyr^{-/-}$ (B6(Cg)-$Tyr^{c\text{-}2J}$/J) retina was unexpected, indicating that it is not contributing to the phenotypic difference present between the two parental strains, but rather, is having its effect masked by other genes. That at least one of those other genes is also present in the QTL is provided by the fact that A.B6-$Tyr^{+/J}$ mice also show an increase in DA cell number relative to the A/J strain. For these mice, the increase cannot be associated with the functional *Tyr* alleles, since they alone are associated with a reduction in DA cell number. Rather, some other polymorphic gene or genes within a 55 Mb region surrounding *Tyr* must also be modulating DA cell number. In addition, bootstrap analysis revealed the consistent

presence of another candidate(s) residing near 67 Mb. Together, their effects should sum to yield (assuming no non-linear epistatic interactions) the phenotypic difference observed in the congenic B6.A<7> chromosome substitution mouse. Polymorphic genes on other chromosomes should in turn combine to yield the entire phenotypic difference between the parental strains, but these did not segregate reliably with the haplotypes associated with this RI strain-set. Some of those, like *Tyr* and *Bax*, may affect multiple types of retinal nerve cell by modulating cellular processes controlling proliferation or survival, while others may act more specifically to set the number of DA cells alone.

We demonstrate a conspicuous role for the *Bax* gene in the control of DA cell number. In conjunction with other studies showing a role for the anti-apoptotic gene *Bcl2*[22], the present results suggest that some of the polymorphic genes modulating DA cell number may do so not only by modulating cell production, but also by modulating cell survival, affecting multiple cell types[22, 24]. No functional polymorphisms were detected within the coding region for the *Bax* gene itself, but a polymorphism in the *Bax* promoter was detected within a p53 consensus binding sequence. p53 is a known modulator of the cellular response following stress and is known to induce *Bax* activation[34], while the polymorphism detected has been shown to affect transcription[25]. Consistent with this, we have confirmed a significant difference in *Bax* expression during postnatal development, with the A/J strain showing higher expression levels, as predicted. Consequently, this variant in B6/J may reduce *Bax* expression levels but is less likely responsible for a dramatic reduction in the number of DA cells since *Bax*+/−mice failed to show any evidence for an effect of gene dosage.

The present results indicate that DA cell number is a complex trait controlled by multiple polymorphic genes, and there are other potential candidates near the *Dacnc7* locus worthy of investigation. The bootstrap analysis indicates a polymorphic gene near 67 Mb. There are three interesting candidates at 78–79 Mb that each contain mis-sense mutations: a gene that codes for aggrecan (*Acan*), a proteoglycan; a gene that codes for hyaluronan (*Hapln3*), a proteoglycan link protein 3; and a gene that codes for milk fat globule epidermal growth factor E8 (*Mfge8*). *Acan* and *Hapln3* are linked in chromosomal location and function[35]. *Acan* is found in developing retina (Popp et al., 2004) and is thought to be important for neural patterning[36] while *Hapln3* interacts with *Acan*[35]. *Mfge8* expression is also found in the retina[37] and is thought to be important for retinal cell adhesion[38], as may *Hapln3* and *Acan*[39]. The recent report that a mutation in the cell adhesion gene *Dscam* increases DA cell density within the mouse retina[40] suggests that cell adhesion molecules might participate in the regulation of DA cell number, encouraging the future pursuit of these as candidate genes.

Far more promising, however, is *Lrrk1*, positioned at the very locus identified in the bootstrap analysis (figure 3b). This gene codes for a leucine-rich repeat kinase 1, is expressed in early neural retina, and is identified as a potential growth regulatory factor[41, 42]. Real time RT-PCR results for this gene showed no significant strain difference in expression levels during postnatal development (not shown), but of the 251 known SNPs discriminating A from B6, six of them are mis-sense mutations (Supplementary Table 3). Most important, *Lrrk1* (a paralog of *Lrrk2*), is linked to the loss of midbrain dopaminergic neurons resulting from familial Parkinson's disease[43, 44], making it a particularly promising candidate for the control of dopaminergic amacrine cells. Indeed, of the candidate genes identified, *Lrrk1* may turn out to be the most specific, modulating exclusively this population of retinal nerve cell.

Supplementary Material

Refer to Web version on PubMed Central for supplementary material.

Acknowledgements

We thank Robin Bishop for assistance with the data collection described in figure 1, and Dr. Lu Lu for genotyping the A.B6-*Tyr*$^{+/J}$ mice. Supported by the NIH (R01 EY-011087; S10 RR-022585)

References

1. Williams RW, Airey DC, Kulkarni A, Zhou G, Lu L. Genetic dissection of the olfactory bulbs of mice: QTLs on four chromosomes modulate bulb size. Behav Genet 2001;31:61–77. [PubMed: 11529276]
2. Seecharan DJ, Kulkarni AL, Lu L, Rosen GD, Williams RW. Genetic control of interconnected neuronal populations in the mouse primary visual system. J Neurosci 2003;23:11178–11188. [PubMed: 14657177]
3. Airey DC, Lu L, Williams RW. Genetic control of the mouse cerebellum: identification of quantitative trait loci modulating size and architecture. J Neurosci 2001;21:5099–5109. [PubMed: 11438585]
4. Peirce JL, Chesler EJ, Williams RW, Lu L. Genetic architecture of the mouse hippocampus: identification of gene loci with selective regional effects. Genes, Brain Behav 2003;2:238–252. [PubMed: 12953790]
5. Zhou G, Williams RW. Eye1 and Eye2: gene loci that modulate eye size, lens weight, and retinal area in the mouse. Invest Ophthalmol Vis Sci 1999;40:817–825. [PubMed: 10102277]
6. Masland RH, Rizzo JF, Sandell JH. Developmental variation in the structure of the retina. J Neurosci 1993;13:5194–5202. [PubMed: 7902864]
7. Raven MA, Eglen SJ, Ohab JJ, Reese BE. Determinants of the exclusion zone in dopaminergic amacrine cell mosaics. J Comp Neurol 2003;461:123–136. [PubMed: 12722109]
8. Williams RW, Gu J, Qi S, Lu L. The genetic structure of recombinant inbred mice: high-resolution consensus maps for complex trait analysis. Gen Biol 2001;2:research0046.0041–0046.0018.
9. Shifman S, Darvasi A. Mouse inbred strain sequence information and yin-yang crosses for quantitative trait locus fine mapping. Genetics 2005;169:849–854. [PubMed: 15520253]
10. Ramakers C, Ruijter JM, Deprez RH, Moorman AF. Assumption-free analysis of quantitative real-time polymerase chain reaction (PCR) data. Neurosci Lett 2003;399:62–66. [PubMed: 12618301]
11. Vandesompele J, De Preter K, Pattyn F, Poppe B, Van Roy N, De Paepe A, Speleman F. Accurate normalization of real-time quantitative RT-PCR data by geometric averaging of multiple internal control genes. Genome Biol 2002;3(7):research0034.0031–0034.0011. [PubMed: 12184808]
12. Hegmann JP, Possidente B. Estimating genetic correlations from inbred strains. Behav Genet 1981;11:103–114. [PubMed: 7271677]
13. Marshall JD, Mu J-L, Nesbitt MN, Frankel WN, Paigen B. The AXB and BXA set of recombinant inbred mouse strains. Mammal Genome 1992;3:669–680.
14. Singer JB, Hill AE, Burrage LC, OOlszens KR, Song J, Justice M, O'Brien WE, Conti DV, Witte JS, Lander ES, Nadeau JH. Genetic dissection of complex traits with chromosome substitution strains of mice. Science 2004;304:445–448. [PubMed: 15031436]
15. Ilia M, Jeffery G. Retinal mitosis is regulated by Dopa, a melanin precursor that may influence the time at which cells exit the cell cycle: Analysis of patterns of cell production in pigmented and albino retinae. J Comp Neurol 1999;405:394–405. [PubMed: 10076934]
16. Rachel RA, Dolen G, Hayes NL, Lu A, Erskine L, Nowakowski RS, Mason CA. Spatiotemporal features of early neuronogenesis differ in wild-type and albino mouse retina. J Neurosci 2002;22:4249–4263. [PubMed: 12040030]
17. Tibber MS, Whitmore AV, Jeffery G. Cell division and cleavage orientation in the developing retina are regulated by L-DOPA. J Comp Neurol 2006;496:369–381. [PubMed: 16566005]
18. Ilia M, Jeffery G. Retinal cell addition and rod production depend on early stages of ocular melanin synthesis. J Comp Neurol 2000;420:437–444. [PubMed: 10805919]
19. Baker GE, Dovey M, Davda P, Guibal C, Jeffery G. Protein kinase C immunoreactivity in the pigmented and albino rat retina. Europ J Neurosci 2005;22:2481–2488.
20. Le Fur N, Kelsall SR, Mintz B. Base substitution at different alternative splice donor sites of the tyrosinase gene in murine albinism. Genomics 1996;37:245–248. [PubMed: 8921397]

21. Knudson CM, Tung KSK, Tourtellotte WG, Brown GAJ, Korsmeyer SJ. Bax-deficient mice with lymphooid hyperplasia and male germ cell death. Science 1995;270:96–99. [PubMed: 7569956]
22. Strettoi E, Volpini M. Retinal organization in the bcl-2-overexpressing transgenic mouse. J Comp Neurol 2002a;446:1–10. [PubMed: 11920715]
23. Péquignot MO, Provost AC, Sallé S, Taupin P, Sainton KM, Marchant D, Martinou JC, Ameisen JC, Jais J-P, Abitbol M. Major role of BAX in apoptosis during retinal development and in establishment of a functional postnatal retina. Develop Dyn 2003;228:231–238.
24. Ogilvie JM, Deckwerth TL, Kundson CM, Korsmeyer SJ. Suppression of developmental retinal cell death but not photoreceptor degeneration in *Bax*-deficient mice. Invest. Ophthalmol. Vis. Sci 1998;39:1713–1720.
25. Semaan SJ, Nickells RW. A polymorphism located in a putative p53 binding site of the murine bax promoter affects transcription: implications of bax as a susceptibility allele in glaucoma. ARVO Abs 2007:#562.
26. Jeon C-J, Strettoi E, Masland RH. The major cell populations of the mouse retina. J Neurosci 1998;18:8936–8946. [PubMed: 9786999]
27. Eglen SJ, Willshaw DJ. Influence of cell fate mechanisms upon retinal mosaic formation: A modelling study. Development 2002;129:5399–5408. [PubMed: 12403711]
28. Tyler MJ, Carney LH, Cameron DA. Control of cellular pattern formation in the vertebrate inner retina by homotypic regulation of cell-fate decisions. J Neurosci 2005;25:4565–4576. [PubMed: 15872104]
29. Rockhill RL, Euler T, Masland RH. Spatial order within but not between types of retinal neurons. PNAS 2000;97:2303–2307. [PubMed: 10688875]
30. Cook JE. Spatial properties of retinal mosaics: An empirical evaluation of some existing measures. Vis Neurosci 1996;13:15–30. [PubMed: 8730986]
31. Rice DS, Williams RW, Goldowitz D. Genetic control of retinal projections in inbred strains of albino mice. J Comp Neurol 1995;354:459–469. [PubMed: 7608332]
32. Ilia M, Jeffery G. Delayed neurogenesis in the albino retina: evidence of a role for melanin in regulating the pace of cell generation. Develop Brain Res 1996;95:176–183.
33. Raven MA, Reese BE. Horizontal cell density and mosaic regularity in pigmented and albino mouse retina. J Comp Neurol 2002;454:168–176. [PubMed: 12412141]
34. Culmsee C, Mattson MP. p53 in neuronal apoptosis. Biochem Biophys Res Comm 2005;331:761–777. [PubMed: 15865932]
35. Spicer AP, Joo A, Bowling RA. A hyaluronan binding link protein gene family whose members are physically linked adjacent to chondroitin sulfate proteoglycan core protein genes: the missing links. J Biol Chem 2003;278:21083–21091. [PubMed: 12663660]
36. McRae PA, Rocco MM, Kelly G, Brumberg JC, Matthews RT. Sensory deprivation alters aggrecan and perineuronal net expression in the mouse barrel cortex. J Neurosci 2007;27:5405–5413. [PubMed: 17507562]
37. Burgess BL, Abrams TA, Nagata S, Hall MO. MFG-E8 in the retina and retinal pigment epithelium of rat and mouse. Mol Vis 2006;12:1437–1447. [PubMed: 17167398]
38. Nandrot EF, Anand M, Almeida D, Atabai K, Sheppard D, Finnemann SC. Essential role for MFG-E8 as ligand for alphavbeta5 integrin in diurnal retinal phagocytosis. Proc Natl Acad Sci 2007;104:12005–12010. [PubMed: 17620600]
39. Popp S, Maurel P, Andersen JS, Margolis RU. Developmental changes of aggrecan, versican and neurocan in the retina and optic nerve. Exp Eye Res 2004;79:351–356. [PubMed: 15336497]
40. Fuerst PG, Koizumi A, Masland RH, Burgess RW. Neurite arborization and mosaic spacing in the mouse retina require DSCAM. Nature 2008;451:470–474. [PubMed: 18216855]
41. Blackshaw S, Harpavat S, Trimarchi J, Cai L, Huang H, Kuo WP, Weber G, Lee K, Fraioli RE, Cho SH, Yung R, Asch E, Ohno-Machado L, Wong WH, Cepko CL. Genomic analysis of mouse retinal development. PLoS Biol 2004;2(9):e247. [PubMed: 15226823]
42. Harada JN, Bower KE, Orth AP, Callaway S, Nelson CG, Laris C, Hogenesch JB, Vogt PK, Chanda SK. Identification of novel mammalian growth regulatory factors by genome-scale quantitative image analysis. Genome Res 2005;15:1136–1144. [PubMed: 16024821]

43. Biskup S, Moore DJ, Rea A, Lorenz-Deperieux B, Coombes CE, Dawson VL, Dawson TM, West AB. Dynamic and redundant regulation of LRRK2 and LRRK1 expression. BMC Neurosci 2007;28:102. [PubMed: 18045479]

44. Taylor JP, Hulihan MM, Kachergus JM, Melrose HL, Lincoln SJ, Hinkle KM, Stone JT, Ross OA, Hauser R, Aasly J, Gasser T, Payami H, Wszolek ZK, Farrer MJ. Leucine-rich repeat kinase 1: a paralog of LRRK2 and a candidate gene for Parkinson's disease. Neurogenetics 2007;8:95–102. [PubMed: 17225181]

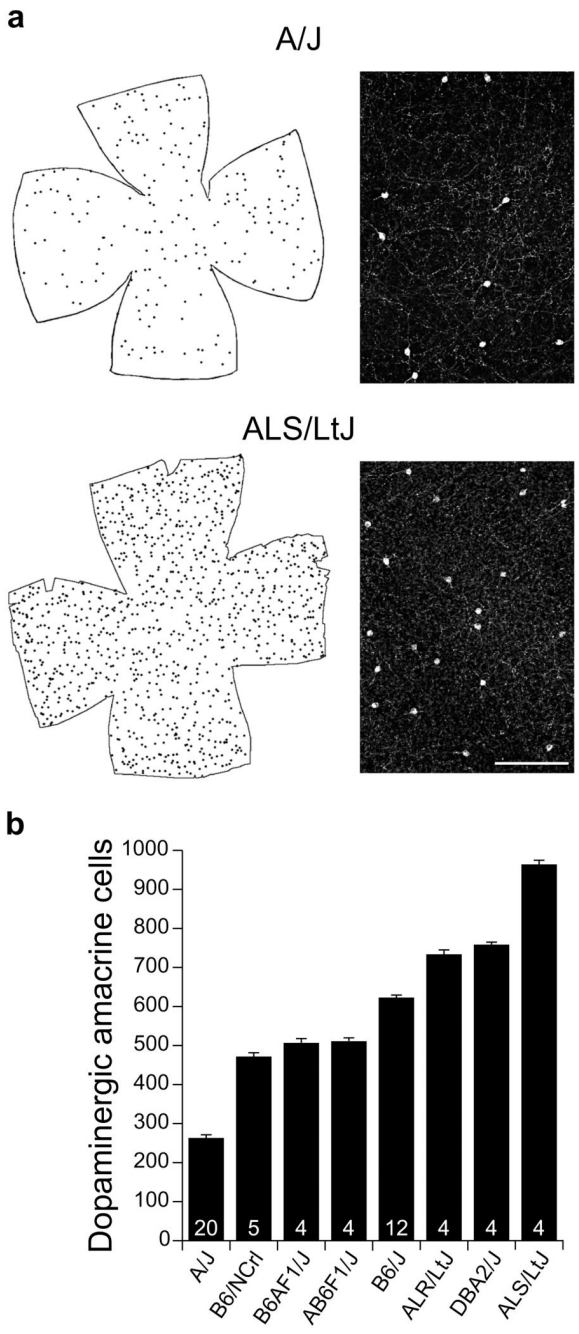

Figure 1.

DA cell number is tightly regulated within a laboratory strain, yet shows substantial variation between strains. a: DA cell distribution in the retina of an A/J mouse and an ALS/LtJ mouse, showing the extremes across these laboratory strains. Confocal images of labeled cells and their processes are shown on the right. Calibration bar = 150 |m. b: Means and standard errors for six laboratory strains as well as the F1 crosses between two of those strains (A/J and C57BL/6J, hereafter B6/J). n = number of mice analyzed per strain, indicated at the base of each bar in the histogram, in this and all subsequent figures.

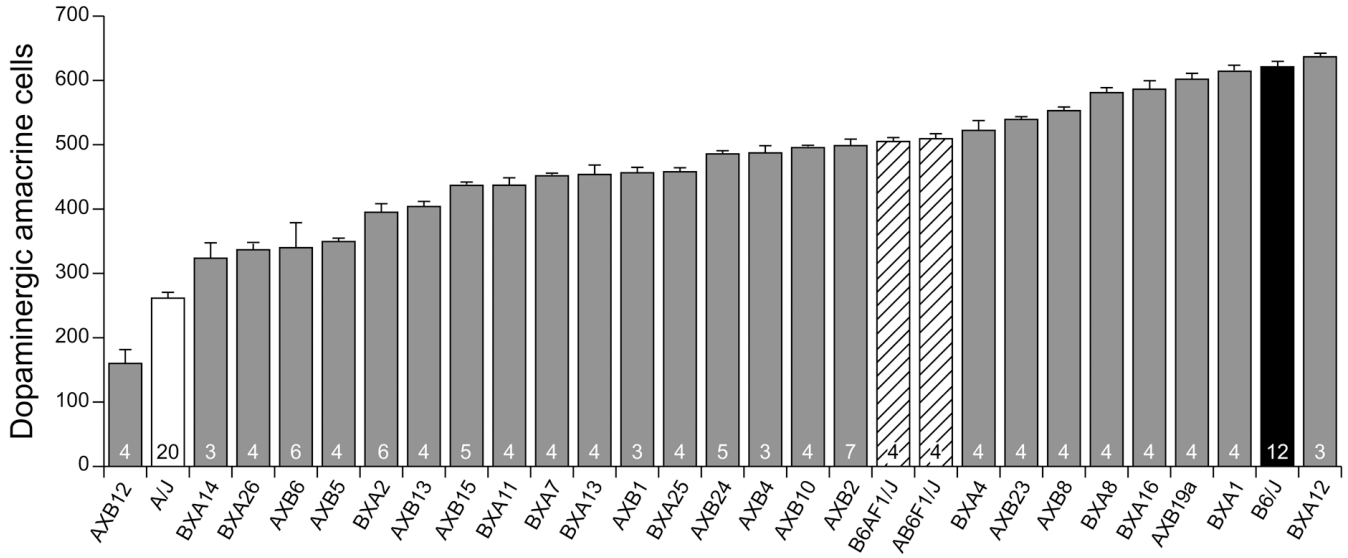

Figure 2.

DA cell number varies across the RI strain-set AXB/BXA (grey bars), suggesting the presence of multiple genes with allelic variants that participate in the control of DA cell number. The parental strains are now (and hereafter) shown in black (B6/J) and white (A/J) for comparison, while the F1 crosses are striped. n = the number of mice analyzed.

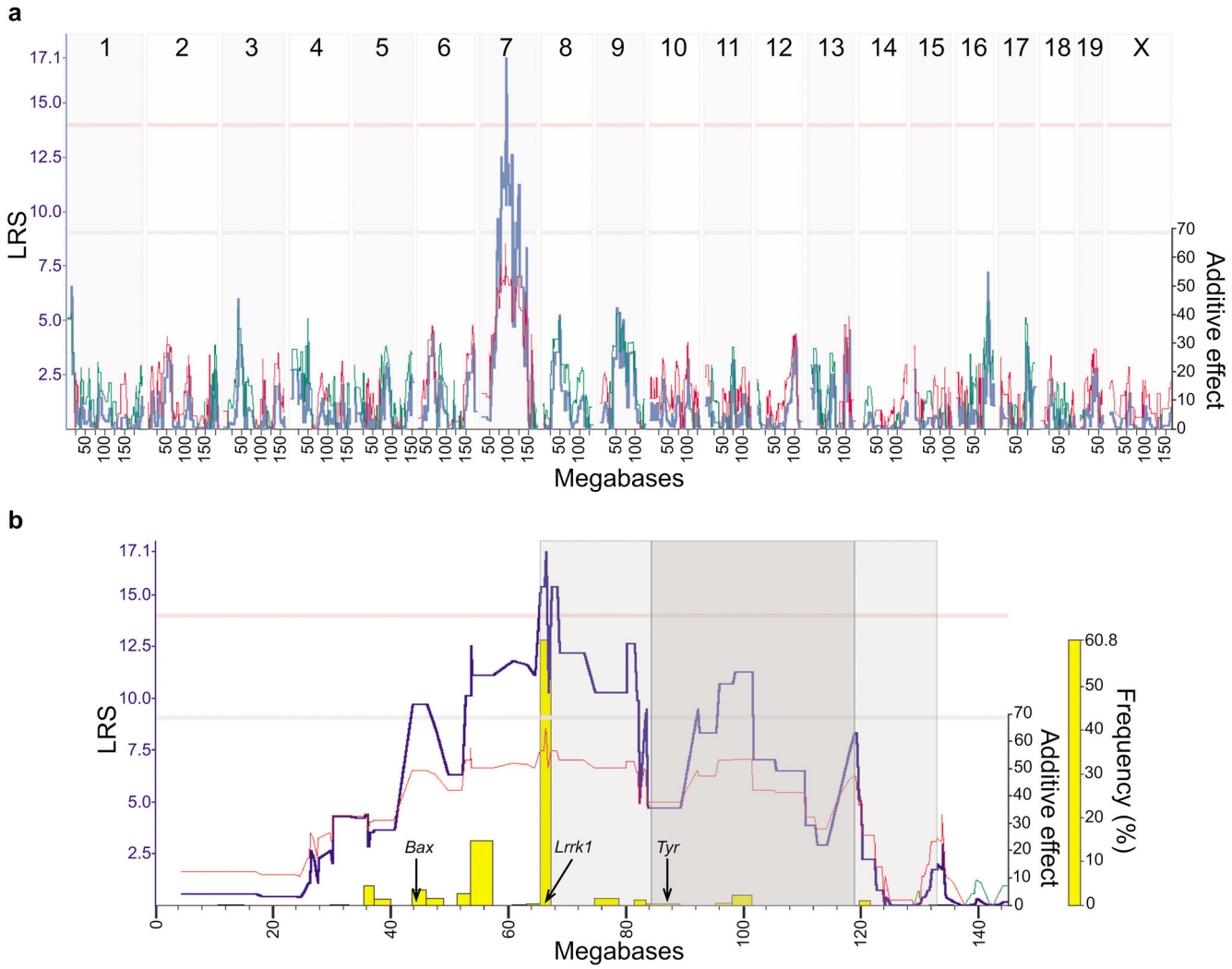

Figure 3.

QTL mapping for DA cell number across the RI strain-set AXB/BXA. a: Whole genome map. The red trace indicates genomic loci where *B* alleles increase trait value while the green trace indicates loci where *A* alleles increase trait value (additive effect, cells per allele; right Y axis). The blue trace indicates the genome-wide likelihood ratio statistic (LRS) associated with the linkage between trait variation and genomic locus. The horizontal lines indicate LRS values associated with suggestive (grey; $p < 0.63$) and significant (pink; $p < 0.05$) effects. b: Chromosome 7 map. The yellow bars show the results of bootstrap testing, revealing the consistent presence of a locus near 67 Mb, where *Lrrk1* is positioned. Also shown are the locations of two other prospective candidate genes that flank this locus, *Tyr* and *Bax*, as well as the introgressed segment of *B* alleles on an otherwise genetically *A* strain background in A.B6-*Tyr*$^{+/J}$ mice (shaded). Lighter shading indicates regions of uncertain haplotype identity. Other conventions as in a.

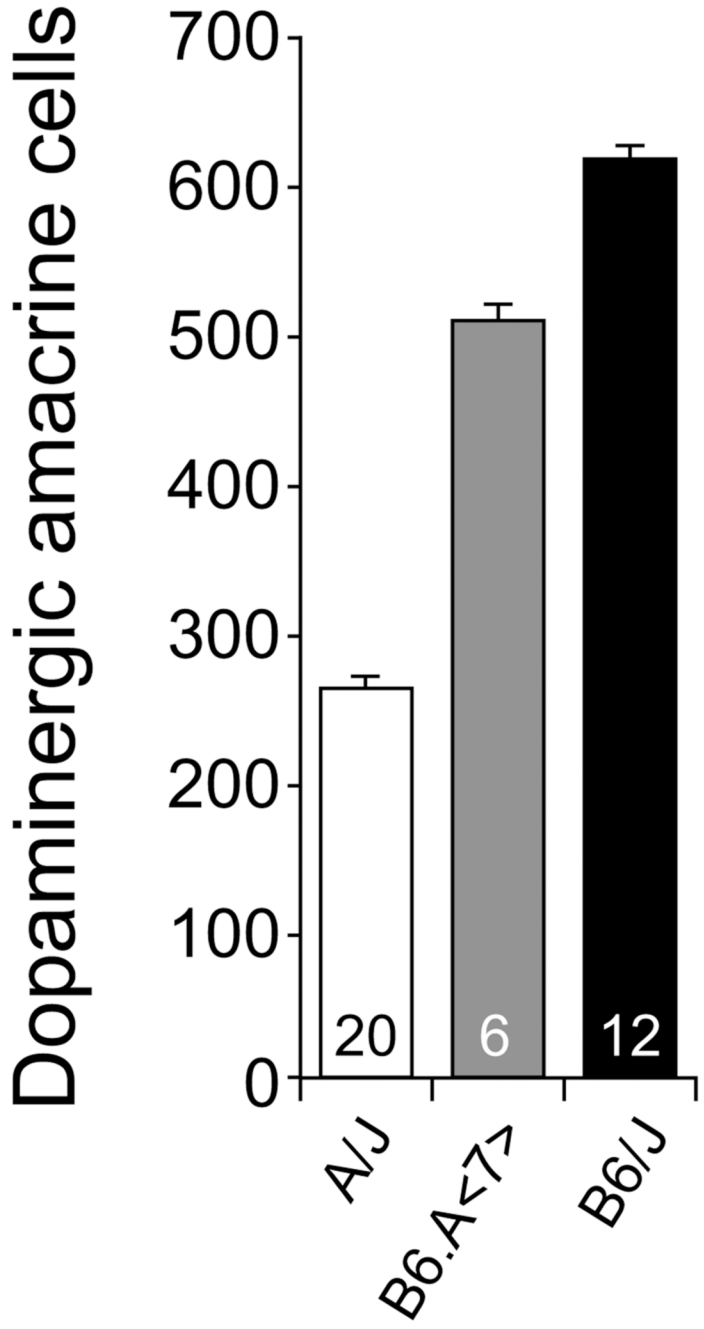

Figure 4.
Consomic mice containing *A* alleles on chromosome 7 contain fewer DA cells. The chromosome substitution strain B6.A<7> had 108 fewer cells than did the B6/J strain, confirming the presence of a QTL on chromosome 7. n = the number of mice analyzed.

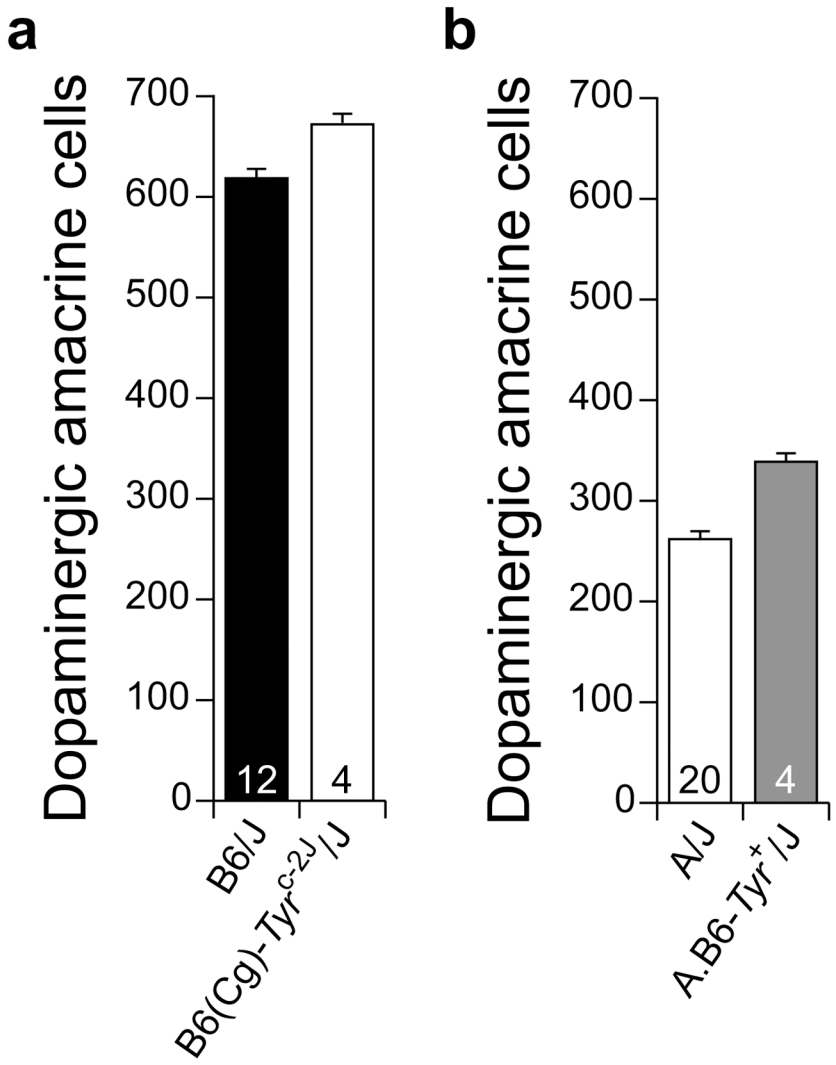

Figure 5.

a: Disrupting a functional *Tyr* gene in the B6/J strain increased DA cell number. b: A.B6-*Tyr*$^{+/J}$ mice contained more DA cells that did A/J mice, indicating that other alleles present in the distal portion of the QTL outweigh any effect of the functional *Tyr* alleles in this retina. Shown, for comparison, in each case in a and b, are the data derived from their comparison laboratory strains, A/J and B6/J, respectively. n = the number of mice analyzed.

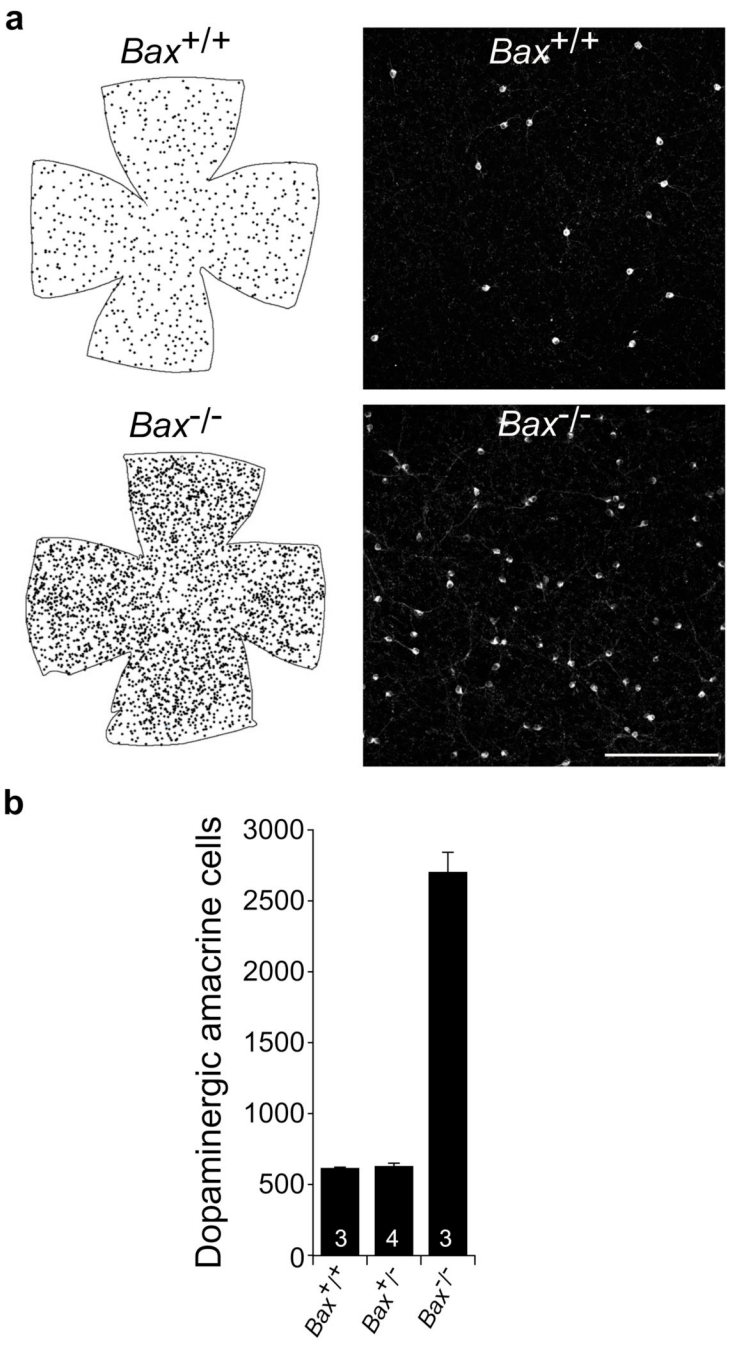

Figure 6.

Bax knockout produces a greater than four-fold increase in DA cell number. a: DA cell distribution in the retina of a $Bax^{+/+}$ mouse and a $Bax^{-/-}$ mouse and associated confocal images. Calibration bar = 200 μm. b: Means and standard errors for $Bax^{+/+}$, $Bax^{+/-}$ and $Bax^{-/-}$ mice. n = the number of mice analyzed.

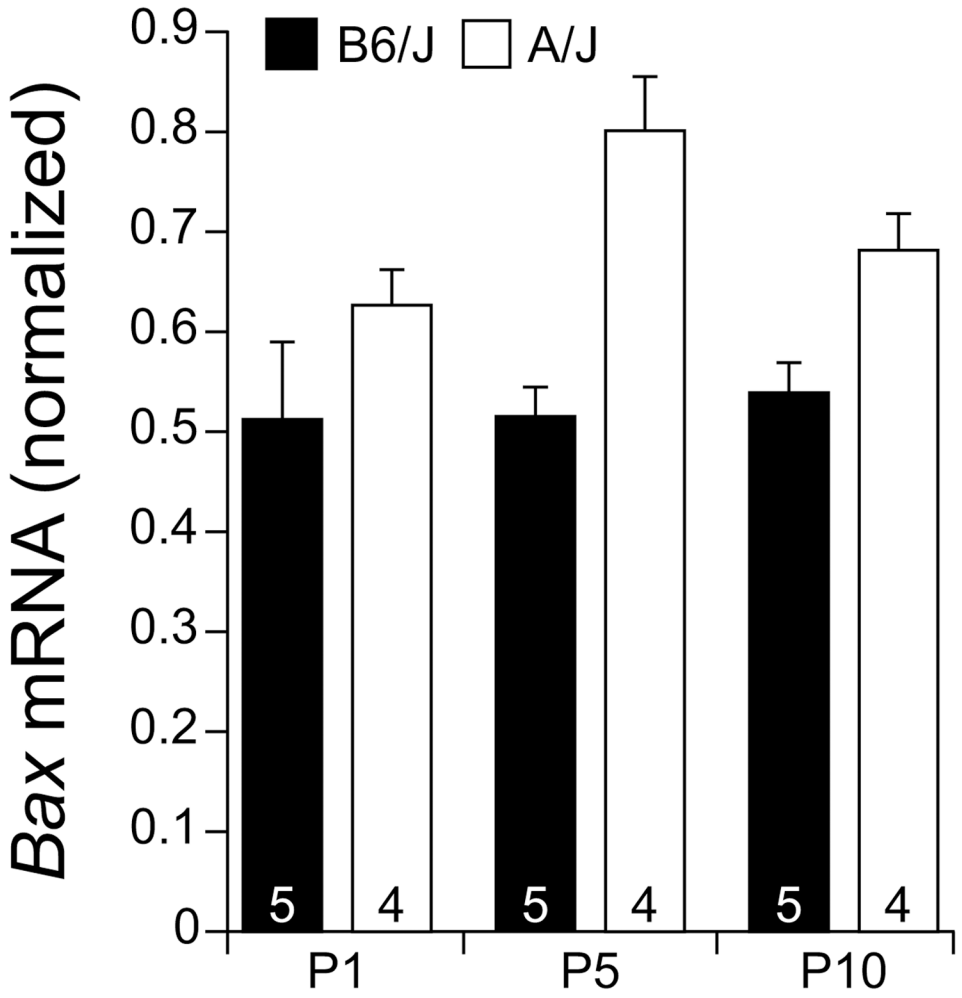

Figure 7.
Bax gene expression during postnatal development differs between the A/J and B6/J strains. n = the number of litters, with each litter consisting of at least three retinas, at P1, P5 and P10, for each strain.